Mansoura Engineering Journal

Volume 39 | Issue 3 Article 10

7-13-2020

Application of Deterministic Lateral Displacement in Biological Cell Separation.

Asmaa Khater
Mansoura University Nanotechnology Center, Egypt, asmaa_elawadhi@mans.edu.eg

Mohamed Sabry
Mansoura University Nanotechnology Center, Egypt, munano@mans.edu.eg

Hossam AbdelMeguid
Mechanical Power Engineering Department., Faculty of Engineering., El-Mansoura University., El-Mansoura 35516., Egypt., hssaleh@mans.edu.eg

APPLICATION OF DETERMINISTIC LATERAL DISPLACEMENT IN BIOLOGICAL CELL SEPARATION

تطبيق الازاحة العرضية المحددة في فصل الخلايا البيولوجية

Asmaa Khater[a,1], Mohamed-Nabil Sabry[a,2], Hossam S.S. AbdelMeguid[b,3]

[a]Mansoura University Nanotechnology Center, Egypt

[b] Mechanical Power Engineering Department, Faculty of Engineering, Mansoura University, El-Mansoura 35516, Egypt

[1] Email: asmaa_elawadhi@mans.edu.eg, Tel.: +201114811461

[2] Email: MuNano@mans.edu.eg, Tel.: +201223169956

[3] Email: hssaleh@mans.edu.eg, Tel.: +201066464712

الملخص العربى

تعتبر عملية فصل الخلايا من العمليات المهمه فى عمليات الفحص المجهرى. توجد عدة طرق لفصل الخلايا بينما يعتبر فصل الخلايا باستخدام جهاز الازاحة العرضية المحدده (DLD)من اكثر الطرق الواعده فى فصل الخلايا حيث ان له عدة مزايا اهمها انه من المستحيل ان يحدث انسداد فى الجهاز. يتكون الجهاز من مجموعه من العوائق يتم ترتيب وضعها ليتم فصل الخلايا طبقا لحجمها. يتم اختيار المسافه بين العوائق بحيث يجب ان تكون اكبر من الحجم الحرج لمنع حدوث انسداد فى الجهاز. فى هذا البحث تم دراسة تاثير كل من قطر العائق و المسافه بين العوائق و كذلك سرعه المائع على الحجم الحرج و من خلال النتائج تم استنتاج معادلة للحجم الحرج كدالة فى مجموعة من المتغيرات اللابعدية.

Abstract

Separation of cells is a crucial operation in most of microbiology tests. It is usually preformed using large sized devices (few tens of cm). In this work, cell separation using a microfluidic device based on Deterministic Lateral Displacement (DLD) is considered. DLD is a promising technique having many advantages, including in particular the fact that it can never be clogged. The device is composed of a micro-channel containing an array of obstacles (also called posts) adequately arranged such as to separate cells based on their size. Distances between posts are much larger than separation size, also called critical size, to prevent clogging. Critical size depends on many design parameters. Many successful designs were published. However, the relation between design parameters and critical diameter has never been systematically explored. Design parameters, geometrical and physical, are numerous. Revealing trends through experiments is impractical, since it requires a large number of cases as well as tedious work to discover relations out of obtained data. In this work, the problem is theoretically analyzed in order to understand the effect of different design parameters and to predict, at least to the first order, separation critical size. Numerous trends are revealed, concerning the effect of velocity, as well as different geometrical characteristics including post size and distances between posts. Finally, a correlation is built giving critical size as a function of dimensionless geometrical characteristics.

Keywords

Bio-MEMs, Cell Separation, DLD Design Parameters, Characteristic Separation Diameter.

Received: 1 August, 2014 - Revised: 7 September, 2014 - Accepted: 7 September, 2014.

1. Introduction

Microfluidic-based devices have recently received large attention as a promising alternative to conventional normally sized devices in the few tens of cm range. Microfluidic devices are not only cheaper, but they are also portable allowing instant medical care. This is a valuable advantage, whether within a medical center or in remote places deprived of such centers. They use less reagent and sample volumes, which reduces environmental impact. They are also more adapted for automation offering less human labor and more accuracy[1-4].

Separation of cells from biological fluids, which is an important step in many biological tests, is an application where bio-MEMs have a high potential. "Deterministic Lateral Displacement" (DLD) [5-7] has been proposed as a promising separation technique, which can never be clogged. In fact, separation surface between cells to be filtered is not a solid surface, but a streamline.

Many studies have implemented this technique experimentally[8-15]. They have reported some success in separating cells. Some design parameters were tested, but values reported were too few to draw general recommendations. To the authors' knowledge, no systematic analysis was made of the effect of all important design parameters. In fact, as of today, there is no available relation that predicts, even to the first order of accuracy, the separation size as a function of design parameters.

The objective of this paper is to study the effect of different design parameters on the size of the separated cells through modeling and simulation. Hence, a rough estimate of expected device performance based on its design parameters will be available, before even building the device, which would be quite helpful for device designers.

Next section will explain the principle of Deterministic Lateral Displacement. The third section will be devoted to problem modeling and simulation techniques. It will be followed by a section in which results are presented and analyzed, before drawing main conclusions in the last section.

2. Deterministic Lateral Displacement Principle

Deterministic Lateral Displacement (DLD) technique is based on continuous streamlines division of biological mixture (Fig. 1) over a bank of obstacles (also called posts), such as to create, at outlet, different zones each having different particle sizes. As it can be seen from Fig. 1 posts are arranged in lines in the y direction (normal to main stream). Posts having their centers on a given line are shifted with respect to posts on the line upstream. The device can have any number of outlets as many as the sizes of the cells need to be separated.

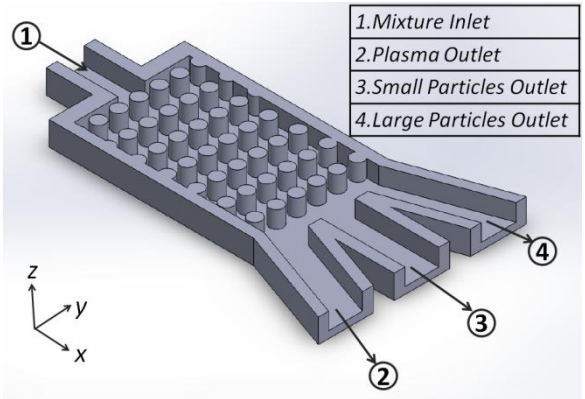

[Figure 1] A 3D Sketch of DLD device

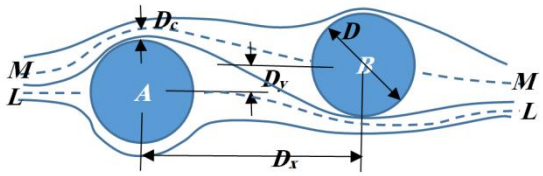

[Figure 2] Deterministic lateral displacement principle

In Fig.2, two posts (A and B), having the same diameter *D*, are placed almost parallel to main stream direction (direction *x*), with a slight shift normal to streamlines (direction *y*). Post displacements (center-to-center) are D_x and D_y, parallel and normal to main stream respectively. Some streamlines are shown, especially those experiencing stagnation, denoted by a dotted line. Streamline LL and MM stagnate at posts A and B respectively. Fluid entering in the stream tube lying between streamlines LL and MM will go above post A and below post B. The smallest thickness ofthis stream tube is, by definition, the critical size S_c. Particles that have a radius that is equal to S_c, or smaller, will remain in the same stream tube along the device. Larger particles willbe displaced to the streamline above. Thus, smaller and larger particles will have different paths. Please note that biological cells are not solid particles. They can be deformed and squeezed to a certain extent into a stream tube that is slightly smaller. The critical size S_c, as defined above, still remains an important property giving the order of magnitude of the dividing line between cells going in one direction and cells going in the other one.

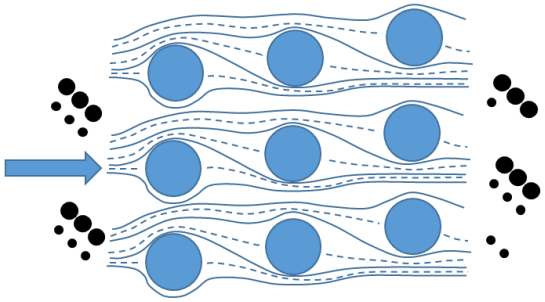

[Figure 3] Bank of posts in a cell separation device

Consider the 3-lines device shown in Fig.3. Between any two posts on the same line passes three stream tubes (delimited by dotted stagnation streamlines). Imagine that in each stream tube enter two particles, one large and one small. Following each particle along the device, small particles will remain in the stream tube while large particles are displaced. So, we will get the distribution shown downstream in Fig. 3. Clearly, larger and smaller particles are concentrated on different sides. This is the principle of DLD devices.

3. Problem Modeling and Simulation

Fluid velocity **v** is usually very small, giving Reynolds numbers (Re, based on fluid velocity v and post diameter D) of the order of 10^{-3}. Hence, a creeping flow model can be used. Device dimension are in the 10 micron – 1mm range. This means that viscous, and hence pressure forces are much greater than gravity, which will be neglected.

Biological fluids are never homogeneous. They contain numerous cells that need to be separated. However, as a first approximation, the concentration of such cells will be assumed rather low, which is the case in many practical applications. In such cases, fluid carrying cells (for instance blood plasma) can be considered as a homogeneous and Newtonian fluid that transports objects that do not perturb main stream. This constitutes the major simplification in this work.

Under such assumptions, governing equations are:

$$\mu \nabla^2 \mathbf{v} = \nabla P \quad (1)$$

$$\nabla \cdot \mathbf{v} = 0 \quad (2)$$

Where**v** is the velocity, μ is the fluid dynamic viscosity and P is the pressure. Problem geometry is that of a 2D channel of width W and length L, in which a certain

number of cylindrical obstacles of circular cross section of diameter *D* are present. Figure 4 presents the case of a channel with two posts. Table 1 gives general characteristics, while Table 2 gives specific characteristics of different test cases. Physical properties were those of blood plasma: kinematic viscosity=$3.3*10^{-6}m^2/s$ and density=1025 kg/m^3.

Table 1 Common geometric features of all test cases

Case No.	*D* (μm)	No. of posts	*Le* (μm)	*W* (μm)	*L* (μm)
1- 12 , 14, 15	30	2	8D = 240	10D = 300	24D=720
13	45	2	8D = 360	10D=450	24D= 1080
16	30	4	10.5D=315	13.5D=390	27D =810

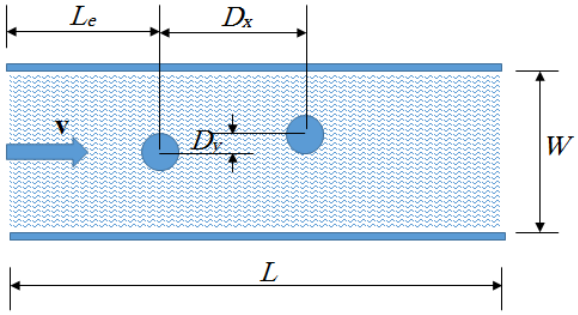

[Figure 4] Channel geometry

Boundary conditions over solid walls (posts as well as channel side walls) are of the no-slip type. A uniform velocity $\mathbf{v}_{in}$ is assumed at channel inlet in the axial direction. Pressure at outlet is assumed to be atmospheric.

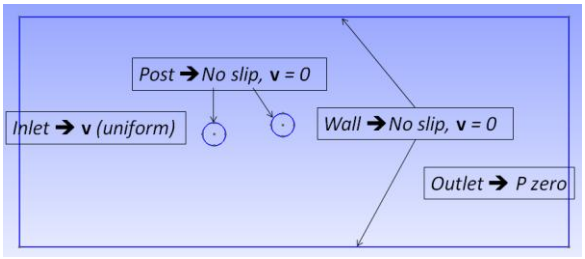

[Figure 5] Simulation boundary conditions

In order to reduce the number of parameters, problem will be cast in a dimensionless form. Post diameter will betaken as the characteristic length. All other dimensionless geometric variables will have the same symbol in small letters. Namely channel width and length are w and l; post displacements are $d_x$and d_y and dimensionless critical size is s_c. Velocity will be scaled by the uniform inlet velocity v_{in}. Pressure will not be scaled by inertia, as usual, because inertia is negligible. It will be scaled by shear stresses, which gives the following dimensionless velocity and pressure (u and p respectively):

$$\mathbf{u} = \mathbf{v}/v_{in} \quad (3)$$

$$p = P\,D/\mu\,v_{in} \quad (4)$$

$$\nabla^2\mathbf{u} = \nabla p \quad (5)$$

$$\nabla\cdot\mathbf{u} = 0 \quad (6)$$

The problem defined above can be solved using the Regular Reductive Integral Method developed earlier[16, 17]. However, solution method is not the focus of this paper, but rather results and their interpretation. A standard solver will be used, which is the open source code Open-Foam (Open Field Operation and Manipulation)[18]. It uses the full Navier-Stokes equation, instead of (5), together with continuity (6). It has an extensive range of features including front tracking of fluid/fluid interfaces, which will be used in a later step to include biological cells.

Table 2Results for different test cases considered

Case No.	D (μm)	No. of posts	D_y(μm)	D_x(μm)	v_{in} (mm/s)	S_c (μm)
1	30	2	0.1D = 3	2D= 60	1.0	3.314
2	30	2	0.1D = 3	3D= 90	1.0	6.200
3	30	2	0.1D = 3	5D=150	1.0	9.260
4	30	2	0.2D = 6	2D= 60	1.0	5.370
5	30	2	0.2D = 6	3D= 90	1.0	9.400
6	30	2	0.2D = 6	5D=150	1.0	14.130
7	30	2	0.4D = 12	2D= 60	1.0	8.500
8	30	2	0.4D =12	3D= 90	1.0	15.700
9	30	2	0.4D =12	5D=150	1.0	23.300
10	30	2	0.2D = 6	2D= 60	1.5	5.370
11	30	2	0.4D =12	3D= 90	1.5	15.700
12	30	2	0.4D =12	3D= 90	5.0	15.700
13	45	2	0.4D =18	3D= 135	1.0	23.500
14	30	2	0.05D =1.5	5D=150	1.0	5.100
15	30	2	0.15D =4.5	5D=150	1.0	12.100
16	30	4	0.4D =12	3D= 90	1.0	15.700

4. Results and Discussion

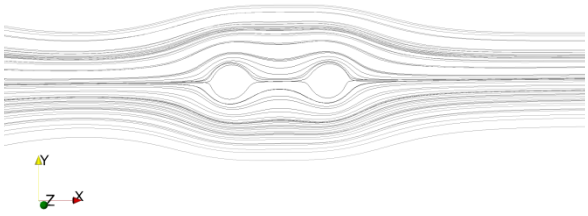

[Figure 6] Streamlines of a sample of simulation cases

Resulting critical sizes are reported in Table 2. It should be noted that identifying the stagnation streamline, which is necessary to obtain the critical size, is rather delicate. In fact, highly accurate identification requires a high resolution in plotting streamlines. It requires a very fine mesh that is impractical. In this work, error in critical size due to insufficient resolution is estimated as ±5%.

Fortunately, there is no need to simulate a whole bank, but only two posts to deduce the critical size in fact the 4-post case (case 16) gives the same results as the corresponding 2-post case (case 8). That is why, for simplicity, only 2-post cases will be studied in the sequel.

From the dimensionless formulation it can be seen that for geometrically similar problems (i.e. same $d_x=D_x/D$ and same $d_y=D_y/D$) then the dimensionless critical size ($s_c=S_c/D$) would be the same. This is made evident by comparing cases 8 and 13.

A little more subtle is the effect of velocity. In fact, velocity amplitude disappears in the dimensionless formulation. This means that the shape of streamlines, which are tangents to the velocity field u, will remain the same for any velocity level. Values of the dimensional stream function on each streamline will depend, of course, on velocity level, but not the streamlines position, which determines the critical size. This is made evident by comparing cases 4 and 10 as well as cases 11 and 12.

Dimensionless shear stress is also independent of velocity level. The latter will obviously have an effect on dimensional

shear stresses. Increasing the velocity would increase the throughput; but it will also increase shear level that may damage cells. Of course in practice cells may be squeezed, especially at relatively high velocities, producing higher pressure and shear. This would have the following effect. The dividing value between large cells and small cells that are being filtered will be a bit higher in practice than the obtained critical size. However, these are secondary effects, slightly modifying results. They will not be considered for simplicity. In a later work, they will be considered by introducing deformable particles.

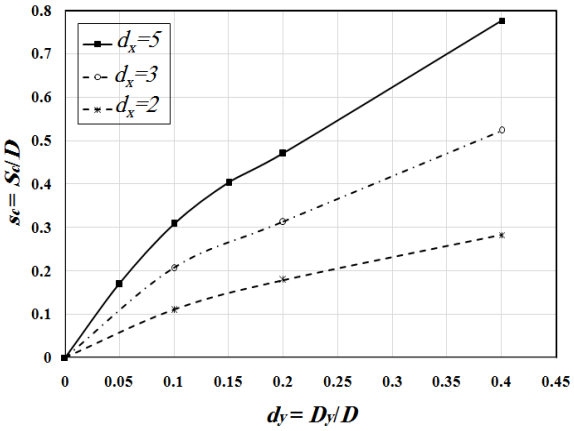

Figure 7Critical size s_c versus shift in the main stream direction d_x and normal shift d_y

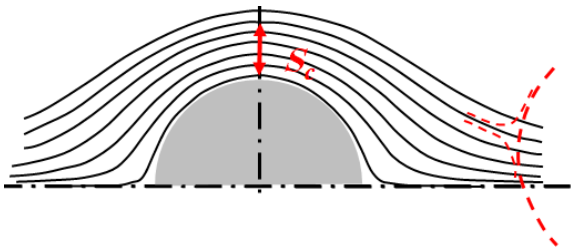

Figure 8 Using streamlines over a single post to understand the effect of different parameters

According to above analysis, dimensionless critical sizes$_c$ depends only on dimensionless shift in the direction of main stream (d_x) and normal to it (d_y), which is plotted in Fig.7. To understand these curves, details of streamlines around a single post in creeping flow are plotted in Fig. 8. Distances between streamlines diminish by approaching the stagnation streamline. Far from it, distances between streamlines tend to stabilize. Imagine a second post (thick dotted line) is placed downstream in a shifted position. For simplicity, first order effect will be considered by assuming second post does not affect streamlines in the upstream zone. One of the streamlines would virtually stagnate over the second post, surrounding streamlines (thin dotted lines) would split in both directions. Stagnation streamline determines the critical size S_c. Assume that the second (virtual) post starts at a certain shift in the mainstream direction D_x and a zero shift normal to main stream D_y=0. Stagnation streamline would be the one that passes by the centerline. At this position Sc=0. Suppose now that the virtual post is shifted normal to mainstream (D_y>0) while keeping the same D_x. At first, streamlines are crossed by the virtual post at a high rate resulting in a rapid increase of S_c, as shows Fig.7. For higher values of D_y, distances between streamlines encountered by the virtual post stabilize, which results in a linear increase of S_c as is shown by Fig.7.

If the experience was repeated at a higher value of shift in the mainstream direction (D_x), we would get a 'similar' curve, although systematically higher than the previous one because streamlines encountered pass at positions that are more distant from the first post (Fig.8).

Based on the fact that curves for different values of d_x in Fig.7 are 'similar', the required correlation will be cast in the form of a product of two functions:

$$s_c = f_1(d_x)\, f_2(d_y) \qquad (7)$$

The first function $f_1(d_x)$ will be selected such as to let $s_c / f_1(d_x)$ be independent of d_x. First of all, such function should contain a factor in the form (d_x – a), a is close to 1,this

is due to the fact that d_x has been defined as the center-to-center distance. To attain similarity, the required function takes the form $f_1(d_x) = (d_x - a)\, d_x^{\,b}$. Best fit (Fig.9) gives:

$$f_1(d_x) = (d_x - 1.1)/\sqrt{d_x}$$

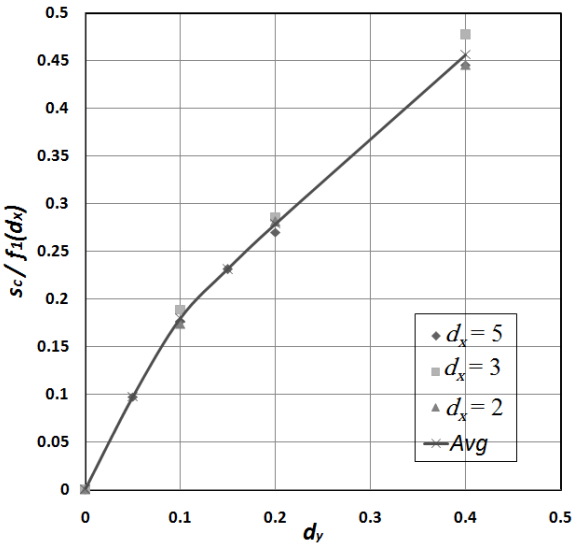

Figure 9 Normalization of s_c by the function $f_1(d_x)$ showing dependence on d_y only.

Figure9 clearly shows that with such normalization, all curves almost coincide. An "average curve" (solid line) of all points available is also shown in the same Figure. The average curve seems to be a good first order estimate of the critical size. The curve starts obviously at the origin and ends asymptotically with a straight line. The shape of $f_2(d_y)$ could thus be a straight line from which is subtracted an exponentially decaying correction function that satisfies the condition at origin. Fitting gives:

$$f_2(d_y) = s_c / f_1(d_x)$$
$$= 0.8844 d_y \qquad (9)$$
$$+ 0.1021\left(1 - \exp^{\left(-d_y(1527 d_y + 7.108)\right)}\right)$$

Table 3 shows that the correlation fits very well the average curve obtained in Fig.9. Relative Error Column was obtained using the correlation form (7) after substituting with f_1 and f_2 from (8) and (9) respectively with a maximum error of 4.4% and an average error of 2.7%.

Table 3Comparing correlation with average results of different displacements (Obtained in Fig.9)

Case No.	Dimensionless s_c	Calculated s_c	Relative Error %
1	0.1105	0.114329	3.496825
2	0.2067	0.197071	4.642841
3	0.3087	0.313336	1.512761
4	0.1790	0.177510	0.832241
5	0.3133	0.305977	2.347719
6	0.4710	0.486492	3.289153
7	0.2833	0.290110	2.391749
8	0.5233	0.500067	4.445818
9	0.7767	0.795087	2.371734
10	0.1790	0.177510	0.832241
11	0.5233	0.500067	4.445818
12	0.5233	0.500067	4.445818
13	0.5222	0.500067	4.445818
14	0.1700	0.170000	2.22E-14
15	0.4033	0.407488	1.030075
16	0.5233	0.500067	4.445818

5. Conclusion

Deterministic Lateral Displacement (DLD) device for cell separation in a liquid stream was theoretically analyzed. The objective was to determine the effect of various device design parameters on its major output, which is the critical size S_c, i.e. the order of magnitude of the size below which particles will be concentrated at one side of device output and above which particles will be concentrated at the other side of it. A major assumption was that transported particles have low concentration and do not affect streamlines.

It was found that:

- Critical size S_c is not affected by the velocity, as long as creeping flow conditions apply
- For geometrically similar devices, *Sc* is proportional to device size, in particular post diameter *D*, i.e. relative critical size S_c is the same for such devices.
- Relative critical size mainly depends on the relative positions of the any two consecutive posts in the main stream direction, but not on the positions of other posts in the bank.
- Relative critical size only depends on two shift components of a post with respect to the position of the post upstream, i.e. the relative shift in the main stream direction $d_x=D_x/D$ and the relative shift in the direction normal to main stream $d_y= D_y/D$, where D_x and D_y are dimensional shift components.
- A correlation was obtained giving relative critical size S_c as a function of relative displacements, d_x and d_y, with an error not exceeding 4.4%, which is in the same range as the resolution error.

References

[1] H. Tsutsui and C.-M. Ho, *Cell Separation by Non-Inertial Force Fields in Microfluidic Systems* vol. 36, 2009.

[2] S. Haeberle, T. Brenner, R. Zengerle, and J. Ducree, "Centrifugal extraction of plasma from whole blood on a rotating disk," *Lab on a Chip,* vol. 6, pp. 776-781, 2006.

[3] D. Mark, S. Haeberle, G. Roth, F. von Stetten, and R. Zengerle, "Microfluidic lab-on-a-chip platforms: requirements, characteristics and applications," *Chemical Society Reviews,* vol. 39, pp. 1153-1182, 2010.

[4] D. Janasek, J. Franzke, and A. Manz, "Scaling and the design of miniaturized chemical-analysis systems," *Nature,* vol. 442, pp. 374-380, 27/07/2006 2006.

[5] L. R. Huang, E. C. Cox, R. H. Austin, and J. C. Sturm, "Continuous Particle Separation Through Deterministic Lateral Displacement," *Science,* vol. 304, pp. 987-990, May 14, 2004 2004.

[6] S. Zheng, R. Yung, T. Yu-Chong, and H. Kasdan, "Deterministic lateral displacement MEMS device for continuous blood cell separation," in *Micro Electro Mechanical Systems, 2005. MEMS 2005. 18th IEEE International Conference on*, 2005, pp. 851-854.

[7] S. Zheng, T. Yu-Chong, and H. Kasdan, "A Micro Device for Separation of Erythrocytes and Leukocytes in Human Blood," in *Engineering in Medicine and Biology Society, 2005. IEEE-EMBS 2005. 27th Annual International Conference of the*, 2005, pp. 1024-1027.

[8] L. Waite and J. M. Fine, *Applied Biofluid Mechanics*: McGraw-Hill, 2007.

[9] H. Mohamed, J. N. Turner, and M. Caggana, "Biochip for separating fetal cells from maternal circulation," *Journal of Chromatography A*, vol. 1162, pp. 187-192, 2007.

[10] D. W. Inglis, J. A. Davis, R. H. Austin, and J. C. Sturm, "Critical particle size for fractionation by deterministic lateral displacement," *Lab on a Chip*, vol. 6, pp. 655-658, 2006.

[11] D. W. Inglis, J. A. Davis, T. J. Zieziulewicz, D. A. Lawrence, R. H. Austin, and J. C. Sturm, "Determining blood cell size using microfluidic hydrodynamics," *Journal of Immunological Methods*, vol. 329, pp. 151-156, 2008.

[12] J. A. Davis, D. W. Inglis, K. J. Morton, D. A. Lawrence, L. R. Huang, S. Y. Chou, J. C. Sturm, and R. H. Austin, "Deterministic hydrodynamics: Taking blood apart," *Proceedings of the National Academy of Sciences*, vol. 103, pp. 14779-14784, October 3, 2006 2006.

[13] D. W. Inglis, N. Herman, and G. Vesey, "Highly accurate deterministic lateral displacement device and its application to purification of fungal spores," ed: American Institute of Physics, 2010.

[14] D. W. Inglis, M. Lord, and R. E. Nordon, "Scaling deterministic lateral displacement arrays for high throughput and dilution-free enrichment of leukocytes," vol. 21, ed: Institute of Physics, 2011, pp. 054024-1-054024-8.

[15] S. H. Holm, J. P. Beech, M. P. Barrett, and J. O. Tegenfeldt, "Separation of parasites from human blood using deterministic lateral displacement," *Lab on a Chip*, vol. 11, pp. 1326-1332, 2011.

[16] M. Sabry, "An integral method for studying the onset of natural convection," *European journal of mechanics. B, Fluids*, vol. 12, pp. 337-365, 1993.

[17] M. N. Sabry, "Sur une nouvelle méthode intégrale et son application aux écoulements de fluides visqueux avec ou sans transfert de chaleur," 1984.

[18] *OpenFOAM The Open Source CFD Toolbox User Guide Version 2.1.0*. (2011). Available: http://www.openfoam.org/archive/2.1.0/docs/user/